Cooperation between level set techniques and dense 3D registration for the segmentation of brain structures

C. Baillard, P. Hellier and C. Barillot
IRISA, INRIA-CNRS unit, Campus de Beaulieu, 35042 Rennes cedex, France
{cbaillar,phellier,cbarillo}@irisa.fr

Abstract

This paper presents a cooperative strategy between volumetric registration and segmentation. The segmentation method is based on the level set formalism. Starting from an initial position, a closed 3D surface propagates towards the desired boundaries through the evolution of a 4-D implicit function. We show that the number of iterations required for convergence is significantly reduced by using a registration process to initialize the surface. Furthermore it makes the segmentation fully automatic. The registration is achieved through a robust multiresolution and multigrid minimization scheme appropriate to our problem. In addition, a bidirectional propagation force depending on local intensity values has been designed for the evolution of the surface. Finally, an adaptive iteration step is automatically computed at each iteration in order to improve the robustness and the efficiency of the algorithm. Results on volumetric brain MR images are presented and discussed.

1 Introduction

The analysis of volumetric brain images has become one of the most important issues for biomedical applications. Segmenting brain structures is crucial to quantify and follow the evolution of many lesions like multiple sclerosis, Parkinson disease (locus niger), Alzheimer disease (hippocampus), cortical atrophy, etc. Research has mainly focused on registration and segmentation [5, 6, 15]. These two problems are closely related, and they can cooperate to take advantage of each other. For instance, automatic segmentation may benefit from registration with an anatomic atlas acting as a template [4], whereas registration can be constrained by a segmentation of cortical structures.

The main difficulties of the segmentation arise from the huge amount of data and from the complexity of anatomical structures. Due to their important variability, these structures can usually not be segmented using registration only, even if this latter is very accurate. The iterative techniques based on the *level set formalism* have proved particularly appropriate for segmenting complex shapes [10, 9, 3]: the detected surface can change topology and cope with significant protusions, and the result is less dependent on initialization than with any other iterative method. However, due to the amount of data involved, the computation time usually required for segmentation is a limit for practical use. Starting from an arbitrary small surface, it may take quite of time to get close to the expected boundaries. Several techniques have been proposed to speed up segmentation [1, 12, 13], but improvement is still required.

In this work, we have been interested in the application of level set techniques for segmenting anatomical structures, and in particular brain structures from MRI. The main contribution of this work is the use of an automatic registration method to initialize the surface. The registration technique is based on a robust hierarchical scheme which can focus on areas of interest [5]. This kind of cooperation has great benefit for the feasibility of the method: the segmentation is faster and completely automatic. Besides, we have extended to the 3D case the design of a bidirectional propagation force which can expand or contract the surface according to local intensity values. Finally, an adaptive step is used for the iterative computation of the surface. The choice of this value is usually manually tuned as a trade-off between speed of convergence and stability of the process, which is hardly compatible with practical applications. We propose to automatically evaluate it at each iteration.

The segmentation method based on level sets is presented in section 2. The use of 3D dense registration for an optimal initialization is explained in section 3. Finally some segmentation experiments with and without cooperation are presented and discussed in section 4. Section 5 presents some concluding remarks and perspectives.

2 3D segmentation based on level sets

2.1 Level set formalism

The segmentation problem is expressed as the computation of a 3D surface $\eta(t)$ (or front) propagating in time along its normal direction $\mathbf{n}$. In the level set formulation [10], the propagating front $\eta(t)$ is embedded as the zero level of a time-varying higher dimensional function $\Psi(\mathbf{X}, t)$:

$$\eta(t) = \{\mathbf{X} \in I\!R^3 \,/\, \Psi(\mathbf{X}, t) = 0\}$$

The function Ψ describes a 4-D surface defined by $\Psi(\mathbf{X}, t) = d$, where d is the signed distance from $\mathbf{X}$ to the front η. The evolution rule for Ψ can be expressed as:

$$\frac{\partial \Psi}{\partial t} + F||\nabla \Psi|| = 0,$$

where F is a scalar velocity function which depends on local properties of the front like the local curvature, and on external parameters related to the input data or expressing an additional propagation force.

The 4D surface Ψ deforms iteratively according to the speed function F, and the position of the 3D front $\eta(t)$ is derived from Ψ at each iteration step by the relation $\Psi(\mathbf{X}(t), t) = 0$. Practically, the function Ψ^{n+1} at step $n+1$ is computed from Ψ^n at step n using the relation:

$$\Psi^{n+1}(\mathbf{X}) = \Psi^n(\mathbf{X}) - \Delta t.F|\nabla\Psi^n(\mathbf{X})|, \quad \forall \mathbf{X} \in I\!R^3 \qquad (1)$$

The next subsections adress the design of F and the choice of Δt.

2.2 Speed function F

The design of the speed function is a key point of the segmentation. Osher and Setian [10] suggest the following:

$$F = h(I)(\nu + \alpha\kappa), \qquad (2)$$

where $h(I)$ is related to the image intensity and acts as a stopping criterion at the location of the desired boundaries, κ represents the local curvature of the front and acts as a regularization term, and ν represents an additional propagation force which makes the surface contract or expand (α is a weighting parameter).

Previous approaches to 3D segmentation using this model have imposed a one-way propagation force ν, which either contracts or expands the whole surface all along the process [16]. However, when the initial position of the surface can be predicted, it is necessary to let the surface evolve in both directions (since predicted and real positions usually overlap). Such adaptive evolution functions have been designed in the 2D case [2, 11, 14]. In eq. (2), the direction of the external propagation force is determined by the sign of ν. Similarly to the 2D approach in [11], this sign is here locally determined by an analysis of local intensity values.

For that purpose, the intensity of the object is modeled by a normal distribution $\mathcal{N}(I_{obj}, \sigma_{obj})$. A threshold value I_{th}, above which a point is more likely to be outside (or inside) the object, has been defined as:

$$I_{th} = \begin{cases} \max\{\ (I_{obj} + I_{bgr})/2,\ I_{obj} + \sigma_{obj}\} & \text{if } I_{obj} < I_{bgr} \\ \min\{\ (I_{obj} + I_{bgr})/2,\ I_{obj} - \sigma_{obj}\} & \text{otherwise} \end{cases}$$

where I_{bgr} is the average intensity of the background limited to a ring around the object. The parameters I_{bgr}, I_{obj} and σ_{obj} are estimated at each iteration using the current segmentation and the associated ring. The propagation force at $\mathbf{X}$ is then defined as:

$$\nu(\mathbf{X}) = \text{SGN}(I_{obj} - I_{bgr}).\text{SGN}(I(\mathbf{X}) - \tilde{I}_{th})$$

where $\tilde{I}_{th}$ is the estimated value of I_{th}. If $I_{obj} > I_{bgr}$, a positive value of $I(\mathbf{X}) - \tilde{I}_{th}$ will induce a positive value for ν, and thus an expanding force ($\mathbf{X}$ is more likely to be *inside* the volume, and Ψ tends to decrease).

The data consistency term suggested in [9] is:

$$h(I) = 1/(1 + \nabla I),$$

where ∇I denotes the gradient of the image. To avoid the contour to stop at spurious gradients, the function $h(I)$ is set to 1 if the closest point on the front belongs to the front for the first time, and if the propagation force ν has not changed its direction since the last iteration [11], since the point is then likely to represent an intermediate location of the surface. It is important for our application since the front can be initially located on any side of the object, where strong gradients can occur.

2.3 Adaptive iteration step Δt

The stability of the process requires a numerical scheme for the computation of $\Delta\Psi$, called *upwind sheme*. The stability is then guaranteed only if the iteration step Δt is limited. This constraint, known as the *CFL restriction* (Courant-Friedrichs-Levy), can be expressed in 3D as:

$$1 \geq \Delta t.(\frac{|H_u|}{\Delta x} + \frac{|H_v|}{\Delta y} + \frac{|H_w|}{\Delta z}),$$

where H is the Hamiltonian defined by:

$$H(u, v, w) = \sqrt{u^2 + v^2 + w^2}.F = F||\Delta\Psi||,$$

with $u = \Psi_x, v = \Psi_y$ and $w = \Psi_z$ [8]. Since we work with a regular sampling grid, we assume $\Delta x = \Delta y = \Delta z = 1$. The maximal value of Δt which guarantees the stability of the numerical scheme is related to the maximal value taken by $|H_u| + |H_v| + |H_w|$ over the domain. Since F is independent from Ψ (see eq. 2), this sum - and therefore Δt - can easily be computed at each iteration.

3 Cooperation with a registration process

The association of the adaptive step with the narrow band technique [1] considerably speeds up the segmentation. However the processing time can be even more reduced (and the segmentation made automatic) if a close and adaptive initialization is provided. In this context information provided by a registration process is of prime interest. Supposing there are N volumes $\mathcal{V}_i$ to be segmented, a reference volume $\mathcal{V}_0$ is chosen and segmented with a manual initialization (a small cube inside the object for instance). Every other volume $\mathcal{V}_i$ (or target) is first registered with the reference one $\mathcal{V}_0$, which provides a dense deformation field (from $\mathcal{V}_0$ to $\mathcal{V}_i$). This field is then applied to the structure detected in the reference volume $\mathcal{V}_0$ in order to predict the location of the structure in the target volume $\mathcal{V}_i$. This prediction is used for initializing the segmentation process.

3.1 Formulation of the registration problem

The registration problem is expressed as a motion estimation problem. The optical flow hypothesis, introduced by Horn et Schunck [7], leads then to the minimization of the following cost function:

$$U(\mathtt{dw}; f) = \sum_{s \in S} [\boldsymbol{\nabla} f(s,t) \cdot w_s + f_t(s,t)]^2 + \alpha \sum_{<s,r> \in \mathcal{C}} ||w_s - w_r||^2,$$

where s is a voxel of the volume, t indexes the volume in the database, f is the luminance function, w is the expected $3D$ displacement field, S is the voxel lattice, $\mathcal{C}$ is

the set of neighboring pairs and α controls the balance between the two energy terms. The first term is the first order Taylor-expansion of the luminance conservation equation and represents the interaction between the field and the data, whereas the second term expresses the smoothness constraint.

The weaknesses of this formulation are known. First, the optical flow constraint (OFC) might not be valid everywhere because of noise, intensity non-uniformity and occlusions; besides discontinuities of the displacement field might not be preserved. Second, the OFC is not valid in case of large displacements because of linearization.

To cope with the first limitation, the quadratic cost has been replaced by robust functions. To face the second one, a multiresolution and multigrid strategy has been designed. More details about the use of robust estimators in the cost function can be found in [5]. The next subsection focuses on the hierarchical aspect of the registration process.

3.2 Multiresolution and multigrid minimization

In order to cope with large displacements, a classical incremental multiresolution procedure has been developed. A pyramid of volumes $\{f^k\}$ is constructed by successive Gaussian smoothing and subsampling. At the coarsest level, the linearization of the conservation equation can be used. At next resolution levels, only an increment $\mathsf{d}\boldsymbol{w}^k$ is estimated and used to refine estimate $\hat{\boldsymbol{w}}^k$ derived from the previous level.

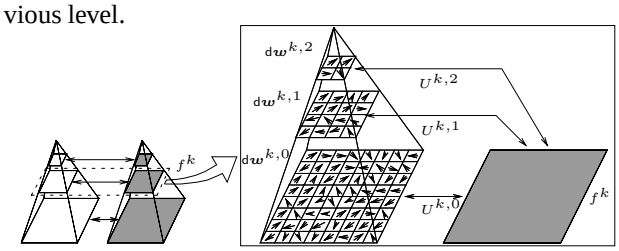

Figure 1. *Example of multiresolution/multigrid minimization. For each resolution level k (on the left), a multigrid strategy (on the right) is performed. For clarity reasons, this is a $2D$ illustration of our 3D algorithm.*

Furthermore, at each resolution level, a multigrid minimization based on successive partitions of the initial volume is achieved (see Fig. 1). A grid level is associated to a partition of cubes. At a given grid level ℓ, a 12-dimension parametric increment field is estimated over each cube of the grid. The resulting field is a rough estimate of the desired solution, and it is used to initialize the next grid level. This hierarchical minimization strategy improves the quality and the convergence rate. The partition at the coarsest grid level is defined using a binary segmentation mask of the structure of interest. Within this work, the mask is provided by the reference segmentation. The octree partition which is thus defined is anatomically relevant. When the grid level changes, each cube is adaptively divided. The accuracy of the registration can therefore be controlled by the accuracy of the final grid level. The final result is a piecewise parametric deformation field.

The hierarchical characteristics of this registration algorithm are appropriate to our segmentation purpose, which only requires a rough and local deformation field. Using the multigrid scheme allows the field to be computed only over areas of interest, i.e., in the neighborhood of the structure to be segmented. In addition, the accuracy of the registration can be limited by stopping the process at a coarse grid level.

4 Experimental results

Experiments have been run on a database of MR images (volume size $256 \times 256 \times 176$). The segmentation of brain ventricles for two different subjects is shown in figure 2. Figure 3 shows the ventricles detected in the reference volume projected onto the target volume, before and after registration. Figure 4 shows the segmentation of the whole brain in the target volume. One 3-D view of the detected ventricles and one 3-D view of the detected brain in the target volume are shown in figure 5.

The segmentation based on level sets provides good accuracy. Protusions of brain and ventricles have been properly recovered, even when the surface has been initialized far away from it (reference volume). Thank to the bidirectional propagation force, the shape is also recovered when initial and expected boundaries overlap (target volume).

No tuning of parameter is required. The iteration step is automatically computed, as well as the threshold on intensity values. The weighting parameter α (eq. 2) has been set to 1, giving small importance to regularization. Using the automatic registration stage, the segmentation is completely automatic. In addition, the number of iterations is considerably reduced: only 170 iterations have been required for segmenting ventricles in the target volume with registration, whereas 580 iterations had been necessary without it. This iteration number decreases from 970 to 240 for the brain segmentation. The time required by the registration algorithm is much smaller than the time saved.

5 Conclusion and further work

The cooperation of level set segmentation and registration has provided very encouraging results. The main contributions are the significant reduction of the iteration number and the complete autonomy of the segmentation process. These results were made possible by the design of an adaptive propagation force and an adaptive iteration step, providing a good trade-off between speed and stability.

We are currently investigating more complex intensity distribution models, in order to extend the method to other applications and other kinds of data. Parameter estimation

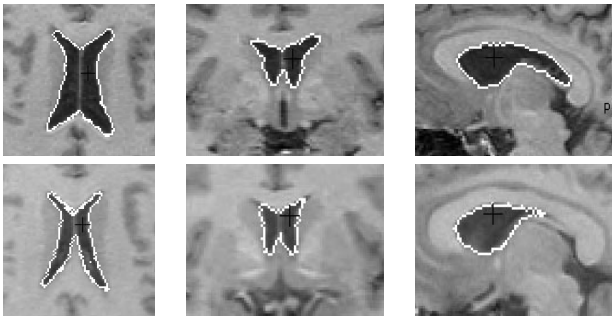

Figure 2. *Ventricle segmentation for 2 different subjects. The first row shows a subpart of the reference volume segmented in 620 iterations (manual initialization with a cube of size $5 \times 5 \times 5$ located inside the ventricles). The second row shows the target volume segmented using the result of the first row, in 170 iterations. The three columns respectively show axial, coronal and saggital planes.*

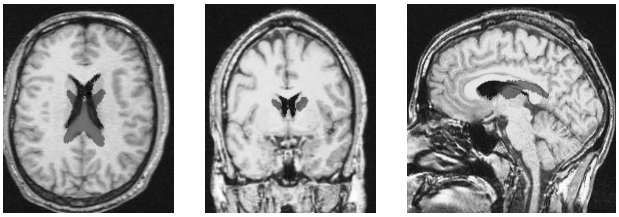

Figure 3. *Ventricules detected in the reference volume projected onto the target volume, before registration (grey) and after registration (black).*

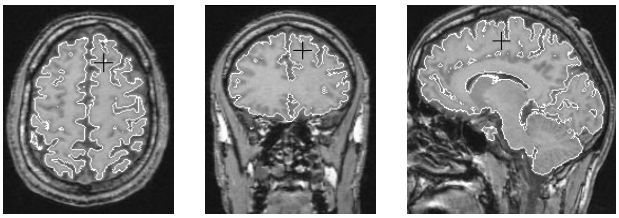

Figure 4. *Brain segmentation in the target volume: the surface was initialized using the registration process, and 240 iterations were necessary.*

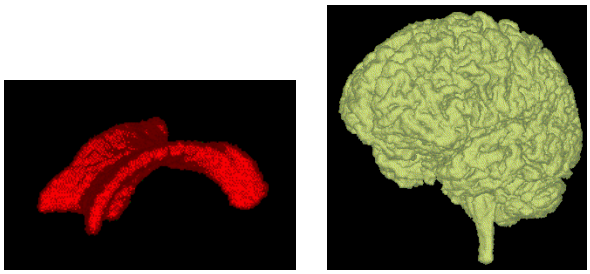

Figure 5. *3D views of the segmented ventricles (left) and brain (right) from the target volume.*

methods (mixture models) could be involved to analyse intensity distributions. The process might also be improved by involving the deformation field in the speed function itself. Finally, reciprocally to this approach, the registration could benefit from the segmentation process.

References

[1] D. Adalsteinsson and J. Sethian. A fast level set method for propagating interfaces. *J. of Computational Physics*, 118(2):269–277, 1995.

[2] O. Amadieu, E. Debreuve, M. Barlaud, and G. Aubert. Inward and outward curve evolution using level set method. In *ICIP*, Kobe, Japan, oct. 1999.

[3] V. Caselles, R. Kimmel, and G. Sapiro. Geodesic active contours. *IJCV*, 22:61–79, 1997.

[4] B. Dawant, S. Hartmann, J.-P. Thirion, F. Maes, D. Vandermeulen, and P. Demaerel. Automatic 3-D segmentation of internal structures of the head in MR images using a combination of similarity and free-form transformations: Part i, methodology and validation on normal subjects. *IEEE Tr. on Medical Imaging*, 18(10):909–916, oct. 1999.

[5] P. Hellier, C. Barillot, E. Mémin, and P. Pérez. An energy-based framework for dense 3d registration of volumetric brain image. In *IEEE Conf. Computer Vision and Pattern Recognition*, Hilton Head Island, South Carolina, jun. 2000.

[6] G. Hermosillo, O. Faugeras, and J. Gomes. Cortex unfolding using Level-Set methods. Technical Report 3663, Inria, apr. 1999.

[7] B. Horn and B. Schunck. Determining optical flow. *Artificial Intelligence*, 17:185–203, auf. 1981.

[8] R. Kimmel, N. Kiryati, and A. Bruckstein. Analyzing and synthesizing images by evolving curves with the Osher-Sethian method. *IJCV*, 24(1):37–55, 1997.

[9] R. Malladi, J. Sethian, and B. Vemuri. Shape modeling with front propagation: A level set approach. *IEEE Tr. on PAMI*, 17(2):158–175, feb. 1995.

[10] S. Osher and J. Sethian. Fronts propagating with curvature dependent speed: Algorithms based on Hamilton-Jacobi formulation. *J. of Computational Physics*, 79:12–49, 1988.

[11] C. Papin, P. Bouthemy, E. Mémin, and G. Rochard. Tracking and characterization of highly deformable cloud structure. In *ECCV*, Dublin, Ireland, jun. 2000.

[12] N. Paragios and R. Deriche. Geodesic active regions for supervised texture segmentation. In *ICCV*, volume 2, pages 926–932, Corfou, Grece, sep. 1999.

[13] R. Whitaker. A level-set approach to 3D reconstruction from range data. *IJCV*, 29(3):203–231, 1998.

[14] A. Yezzi, A. Tsai, and A. Willsky. Binary and ternary flows for image segmentation. In *ICIP*, Kobe, Japan, oct. 1999.

[15] X. Zeng, L. Staib, R. Schultz, and J. Duncan. Segmentation and measurement of the cortex from 3D MR images using coupled surfaces propagation. *IEEE Tr. on Medical Imaging*, 18(10):148–157, oct. 1999.

[16] X. Zeng, L. Staib, R. Schultz, H. Tagare, L. Win, and J. Duncan. A new approach to 3D sulcal ribbon finding from MR images. In *MICCAI*, pages 148–157, sep. 1999.